A Platinum Open Access Journal for Organic Chemistry

Paper

Free to Authors and Readers | DOAJ Seal | *Arkivoc* **2024** (7) 202412263

Identification of local benzenoid aromaticity and global aromaticity of polycyclic aromatic hydrocarbons (PAHs) *via* the corresponding ring current effects in ^{1}H NMR spectroscopy

Erich Kleinpeter* and Andreas Koch

Chemisches Institut der Universität Potsdam, Karl-Liebknecht-Str. 24-25, D-14476 Potsdam (OT Golm), Germany

E-mail: ekleinp@uni-potsdam.de

In memory of Paul von Ragué Schleyer, the discoverer of NICSs, who passed away 10 years ago

Received 07-24-2024 **Accepted** 10-14-2024 **Published on line** 11-17-2024

Abstract

The spatial magnetic properties of aromatic compounds, through-space NMR shieldings (TSNMRSs, actually the ring current effect in ^{1}H NMR spectroscopy), of a selection of polycyclic aromatic hydrocarbons (PAHs) have been calculated using the GIAO perturbation method employing the Nucleus Independent Chemical Shift (NICS) index and visualized as Iso-Chemical-Shielding Surfaces (ICSS) of various size and direction. The deshielding belt in-plane of the aromatic moieties and around the periphery of PAHs unequivocally verifies the aromaticity of PAHs at first glance. The shielding areas above/below the plane of mono- and polycyclic aromatic moieties and/or the whole PAH characterize the extent of detectable aromaticity. Deshielding areas found at the center of the non-aromatic moieties are the internal contributions of the deshielding belt. This creates a holistic representation of the aromaticity of PAHs.

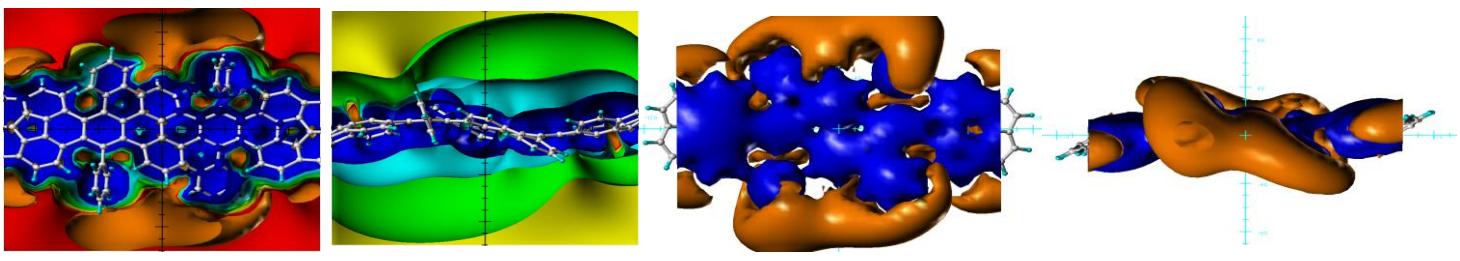

Keywords: PAHs; Aromaticity; NMR; NICS; TSNMRS

Introduction

Polycyclic aromatic hydrocarbons (PAHs) often have unique optoelectronic properties and, therefore, are for this reason often found as components of organic electronics as are light emitting diodes, transistors and photovoltaic cells. Their optical properties are significantly dependent on structure and properties of the PAHs, which depend not insignificantly on the local aromaticity of the individual rings and/or the global aromaticity of the complete PAH. Relationships between the optical properties and the aromaticity of PAHs are largely empirical and depend essentially on the extent of (anti)aromaticity(ies). The desired optical properties of the PAHs thus determine the synthesis options and, among other requirements, considerably the aimed aromaticity of the PAHs.

PAHs are structurally polycyclic conjugated hydrocarbons; they are planar, in case of additional four- and/or five-membered ring moieties and/or steric hindrance they deviate from planarity. Most of the available six-membered ring moieties of PAHs are usually aromatic (dominated and classified by Clar´s π-electron sextets),[1] but could also be non- or even assigned to be anti-aromatic. Relevant information about the local and/or global aromaticity, non- or antiaromaticity is usually provided by theoretical calculations of the corresponding causal local, global or peripheral ring currents[2–5] (vector maps are created in which arrows indicate direction and intensity of the in-plane current and contours/shading the total magnitude); anticlockwise (clockwise) circulations represent paratropic (diatropic) ring currents. At the same time and/or alternatively a NICS[6,7,8] analysis is performed [NICS(0), NICS(1), NICS(1)$_{\pi,zz}$ values in plane or 1 Å above plane in the ring center or the corresponding scans].[9-14] NICS(1)$_{\pi,zz}$ parameters[16] and scans consider only the π-components of the NICS parameters and thus are in direct linearity with the corresponding ring currents.[5] The final information is existing aromaticity (−NICS$_{\pi,zz}$ values), antiaromaticity (+NICS$_{\gamma,zz}$ values), local/global/peripheral dia- and para-tropic ring currents, respectively.

Along the NICS analysis, only individual NICS values or NICS sans, in the centre and/or 1 Å above ring centre(s), are utilized;[9-14] further in-plane information inside the individual rings of PAHs or outside around the PAH molecules is available *but not yet taken into account.* In the NICS-X and NICS-XY scans[14] the calculations are extended beyond the molecules, however, the deshielding areas outside the molecules they are not considered yet and therefore not taken into account. Coquerel and co-workers[15] also calculated more-dimensional visualizations of PAHs 1 Å above the van der Waals surface of the molecules, but here the range from +5.5 to −5.5 ppm was also not taken into account, not differentiated and all shown in gray.

Instead, we have a method in hand that takes into account, quantitatively differentiates and displays the entire 3D spatial information[16–20] about existing dia- and paratropic regions of the ring current effect of aromatic compounds in ^{1}H NMR spectroscopy *outside and not only 1 Å above the PAHs*; the latter information outside the molecules, especially the *in-plane deshielding belt of aromatic structures*, has been neglected so far and has not yet been included in the classification of PAHs but proves to be essential (*vide infra*).[16–20]

To achieve and differentiate the comprehensive 3D spatial information of the magnetic properties, *i.e.* the ring current effect in the ^{1}H NMR spectra of PAHs, is the reason for this study. This amounts to a holistic view of the spatial magnetic properties, which not only indicate the π-driven ring current on site, but reflects the aromaticity of the PAHs as a whole on the magnetic point of view.

Results and Discussion

We employed our through-space NMR shielding (TSNMRS) concept[16–20] to qualify and quantify the spatial magnetic properties (actually the ring current effect in ^{1}H NMR spectroscopy) of some selected PAHs. Along with our concept, the chemical shifts (NICS values) are calculated for a grid of ghost atoms surrounding the molecules in order to locate diatropic and paratropic regions inside and around the PAHs. The TSNMRSs are visualized as iso-chemical-shielding surfaces (ICSSs) of various size and direction and are employed to qualify and quantify the ring current effects of the studied PAHs − experimental Δδ/ppm values in the corresponding ^{1}H NMR spectra of the studied PAHs are *the molecular response property of our TSNMRS values*.[19,20]

As prime examples of PAHs, five compounds were first selected that were recently synthesized and also examined for their aromaticity by NMR spectroscopy; they have been calculated [see experimental section; structures are given in (Scheme 1)] and studied for their aromaticities on the magnetic criterion.

1

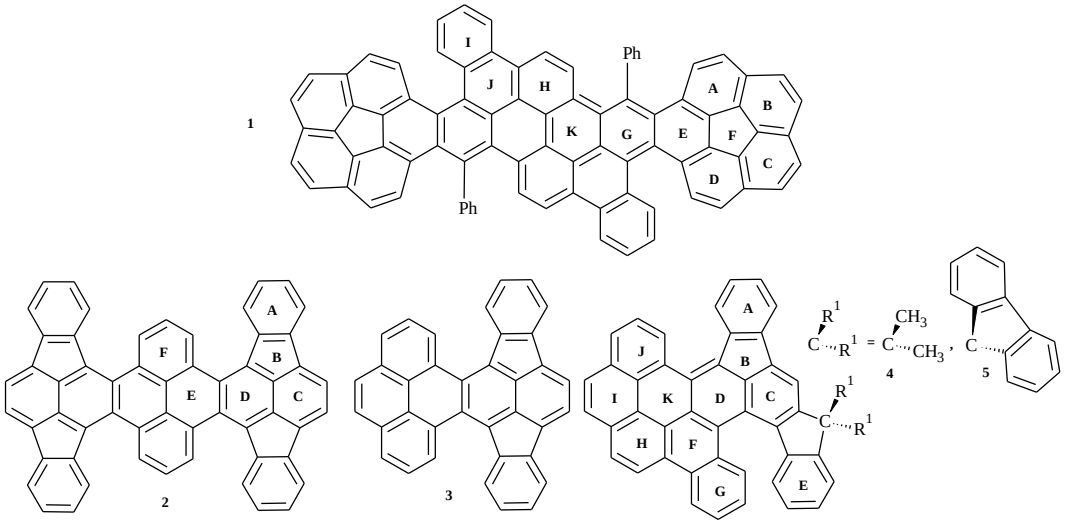

Scheme 1. Polycyclic aromatic hydrocarbons (**1–5**) studied.

The distorted hybrid corannulen dibenzo*bis*tetracene **1** was recently synthesized by the group of Hua Jiang[21] and the obtained results on the magnetic criterion [NICS(1)$_{\pi,zz}$ study and plots of the anisotropy of the induced ring current(s)[23]][21] have been compared by Dickens and Mallion with the quasi graph-theoretical Hückel−London−Pople−McWeeny (HLPM) method[3] of calculating π-electron ring currents.[22] The two five-membered rings of **1** were assigned to be substantially anti-aromatic, the six-membered rings to have different aromaticity (from non- *via* reduced up to inevitably, entire aromaticity around the global perimeter of the PAH);[21,22] depending on the position in the molecule; differences in the aromaticity of present 6-membered rings are observed.[21,22]

The corannulene dibenzo*bis*tetracene **1** is not planar, rather slightly curved like a wave, the terminal corannulene units are bowl-shaped;[14] due to steric hindrance the freely rotating phenyl moieties are perpendicular to the core molecule and their π-electron sextets, inevitably not included in the π-delocalization of the core molecule. The ring current effects of **1** (TSNMRSs of different size and direction) are given in various visualizations by the ICSS(+5ppm) (blue, *shielding*) and ICSS(−0.5 ppm) (orange, *deshielding*) in *Figure 1*. The expected profile for a polycyclic aromatic hydrocarbon is apparent at first glance (compare with

benzene in *Figure 1*, *right, below*): Shielding above/below the ring plane, deshielding in plane, both qualitatively indicated by size and direction of δ(^{1}H)/ppm of the corresponding protons.[24,25]

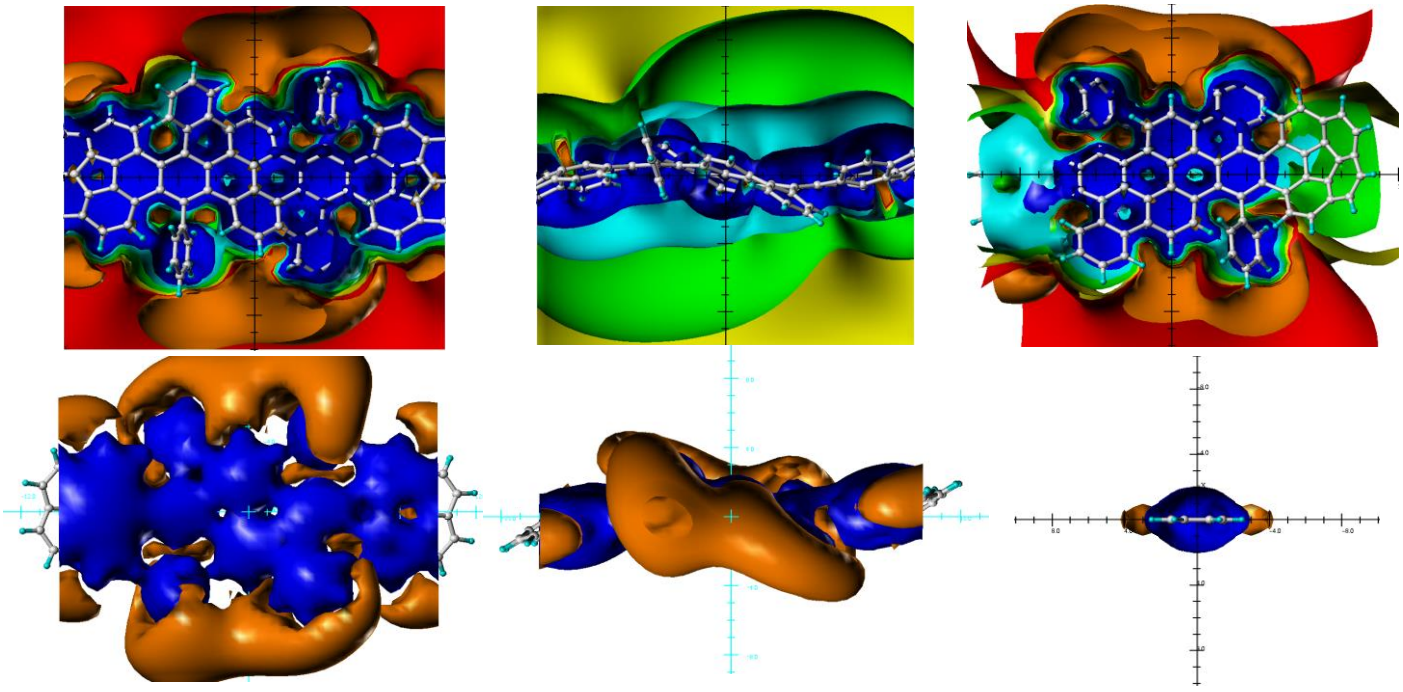

Figure 1. Visualisation of the spatial magnetic properties (TSNMRSs) of **1** (in various views) and the side view of **benzene** (*left, blow*) by different ICSS of −0.5 (orange) and −0.1 ppm (red), *deshielding* and 5 ppm (blue), 2 ppm (cyan), 0.5 ppm (green) and 0.1 ppm (yellow) *shielding*.

The in-plane deshielding belt [ICSS(−0.5 ppm) (orange)] is particularly characteristic and unequivocally classifies the aromaticity of the PAH **1** as a whole and the benzenoid aromaticity of the aromatic π-sextet ring moieties on the edge. This deshielding zone outside around the aromatic molecule is in case of **1** not closed, but partially covered by the strong shielding effects above/below the ring planes, because the extent of the ICSS(−0.5 ppm), *deshielding* is only a tenth as strong as the *shielding* zone ICSS(+5ppm).

The benzenoid aromaticity of the individual rings on the edge is also clear in the interior of the molecule: Due to the benzene-diction-identical ring current effect [ICSS(+5ppm) (blue, *shielding*)] the rings A, B, C, D, G, H and I are aromatic, the remaining rings J, K and E are not aromatic (as are the symmetry-related analogues). Finally, the five-membered rings in the terminal corannulene moieties of 1, which were classified as anti-aromatic in both previous papers:[21,22] The corresponding ring current effect above/below the plane of these five-membered rings proves to be deshielding, however, of about the same size as in the deshielding belt [ICSS(−0.5 ppm) (orange, *deshielding*)] outside the molecule. From this, it can be concluded that the assumed antiaromaticity of the 5-membered rings[21,22] is actually non-aromaticity and that the existing deshielding zone is only the inner-molecular part of the paratropic deshielding belt in **1**. This deshielding effect is more pronounced than in the non-aromatic 6-membered rings J, K, and E, but here the deshielding belt is effective on a smaller number of adjacent aromatic rings than on five 6π-benzenoid rings in the terminal corannulene moieties of **1**.

Just as clearly demonstrable from the ring current effects is the evidence of local and global aromaticity of double and quadruple [5]helicenes **2**, **3** and π-extended [*n*]helicenes **4** and **5** (Scheme 1). The compounds have been synthesized and structurally characterized by Wei et al.;[26] the aromaticity assessment of **2–5** is

limited to the antiaromaticity comparison of the 5-membered rings contained in the compounds: The antiaromaticity in **2** and **3** [NICS(0) = 9.37 and >9.13, respectively] was found to be substantially higher than in **4** and **5** (NICS(0) = 5.75 and 5.63, respectively).[26]

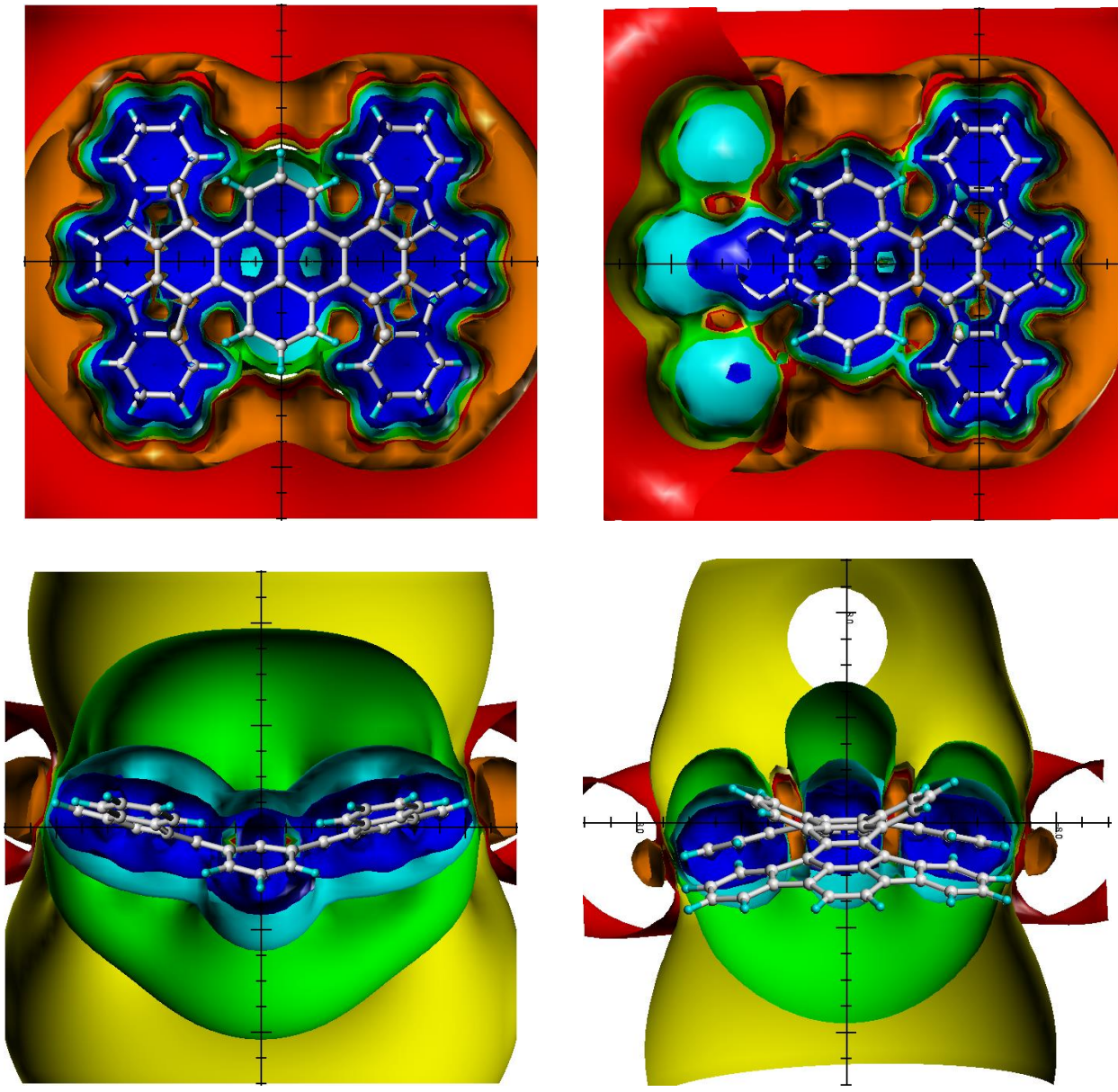

Figure 2. Visualisation of the spatial magnetic properties (TSNMRSs) of **2** (top views above; side views below) by different ICSS of −0.5 (orange) and −0.1 ppm (red), *deshielding* and 5 ppm (blue), 2 ppm (cyan), 0.5 ppm (green) and 0.1 ppm (yellow), *shielding*.

The helicene derivatives **2–5** are due to steric hindrance and present five-membered ring moieties not planar, instead slightly wavy but still highly conjugated. The TSNMRS values [ICSS(−0.5) and (−0.1 ppm) orange and red *deshieldung*, and ICSS(+5 ppm) blue, (+2 ppm) cyan, and ICSS(+0.5 ppm) green *shielding* have been evaluated] unequivocally prove **2–5** to be PAHs (shielding ICSSs above/below the plane of the various ring moieties and the dominant complete deshielding belt (Figures 2 and 3; compounds **2** and **4** are given, **3** and **5** see Supporting Information). The suggested peripheral ring current[26] is not detectable, but the individual benzenoid ring moieties exhibit their own local and overlapping ring current effects. If the aromatic benzenoid

rings in the structures of **2–5** are adjacent and behave like phenanthrene or naphthalene subunits on the magnetic criterion, the ring current effects combine to form common representations such as those known from the corresponding aromatic hydrocarbons, respectively.[17,18]

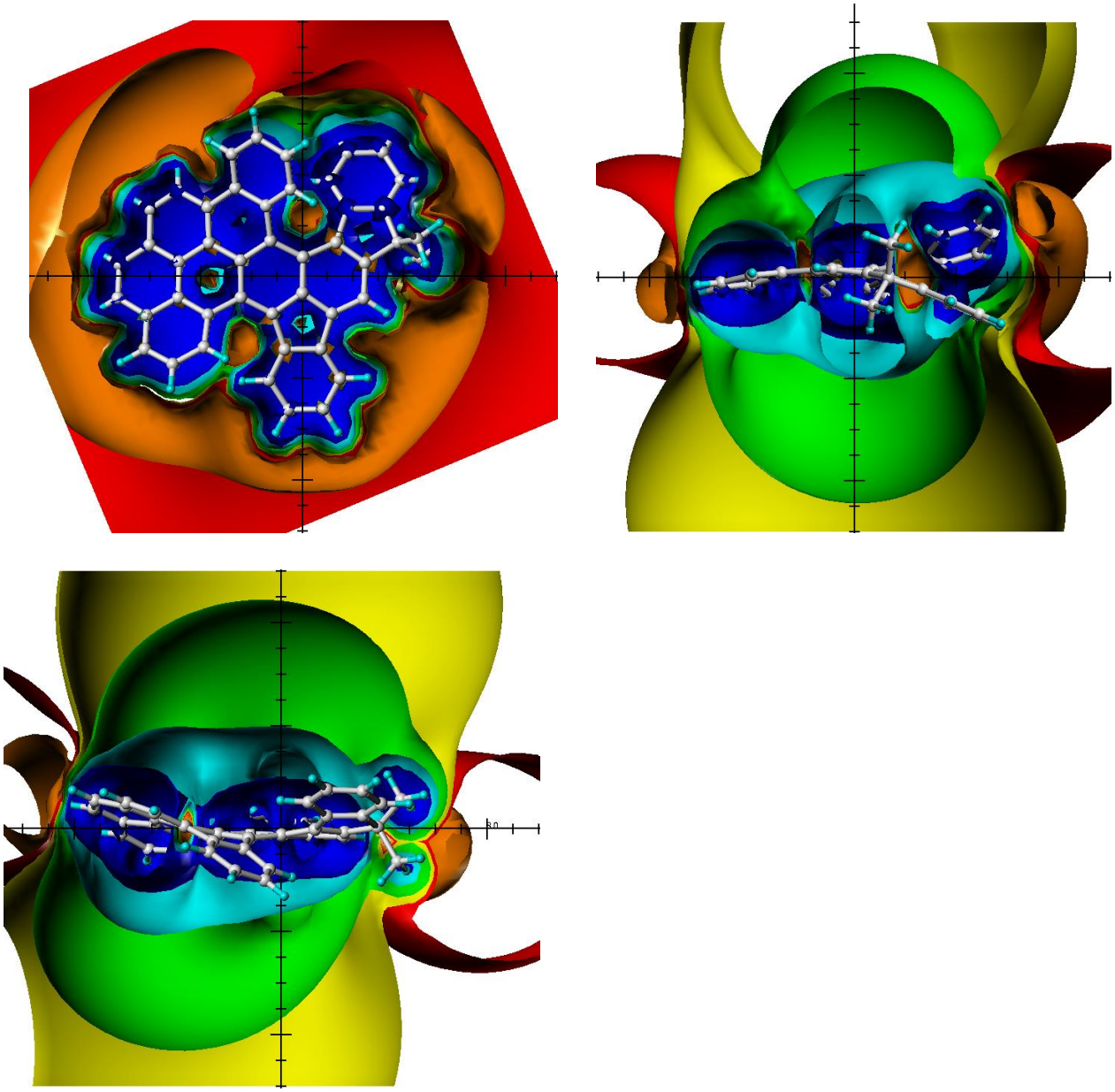

Figure 3. Visualisation of the spatial magnetic properties (TSNMRSs) of **4** (top view above; side views below) by different ICSS of −0.5 (orange) and −0.1 ppm (red) *deshielding* and 5 ppm (blue), 2 ppm (cyan), 0.5 ppm (green) and 0.1 ppm (yellow) *shielding*.

The conjugated 6π-aromatic benzenoid ring moieties A, C, D and F (**2** and **3**) and A, C, D, E, G, H, I, J (**4** and **5**) exhibit the same ring current effect as benzene, however, the six-membered ring moieties E (in **2**, **3**) and F, K (in **4** and **5**), as well as the five-membered ring moieties B in all four compounds deviate from this. They are non-aromatic: In the case of the 6-membered rings, the inner deshielding belt zone is covered by the shielding ICSSs above/below plane; within the 5-membered ring moieties it is visible in the expected size.

There are no major deshieldings above/below plane that could indicate partial antiaromaticity of the E and B moieties, respectively.

Another two corannulene-based PAHs **6** and **7** have been synthesized by Qi Xu et al.[27] (Scheme 2) and both global and local aromaticity was investigated by a $NICS_{\pi,zz}$ study[9-14] and using the Anisotropy of the Induced Current Density (ACID) calculation[23] of potential ring currents.[27] The additional five-membered ring M in **7** as the five membered rings F of the corannulene units in **6** and **7** were found anti-aromatic, the benzene rings all to be aromatic except the central six-membered rings H and L, respectively, which were non-aromatic.[27] The calculated ACIDs are in agreement with the $NICS_{\pi,zz}$ calculations.[27]

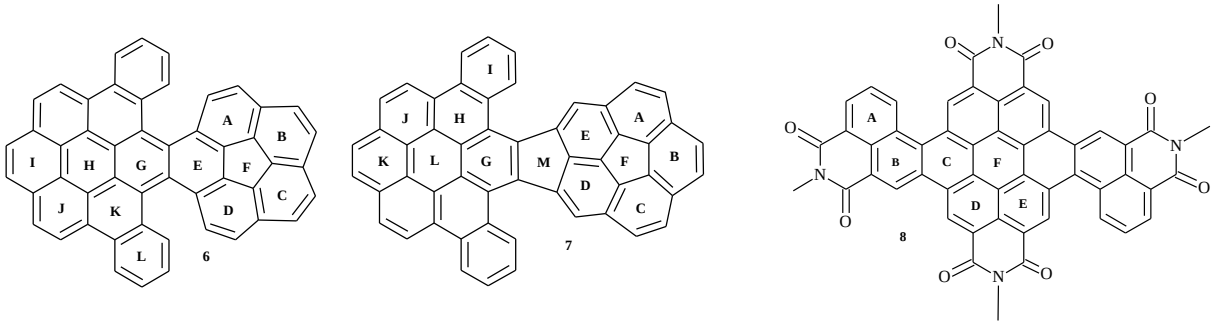

Scheme 2. Polycyclic aromatic hydrocarbons **6–8**.

The TSNMRS visualization of the spatial magnetic properties of **6** and **7** on the magnetic criterion are given in Figure 4. Like the former molecules and for the same reasons are the coroannulene/coronene derivatives **6** and **7** bent like a bowl; thus, it is not so easy to represent three-dimensionally local and the global ring current effects of these PAHs: However, the strong shielding ring current effect above/below the bowl-like surface and the expressive deshielding belt in-plane around the complete molecules are unequivocally indicated. The continuous ICSS (+5 ppm) of the aromatic rings is only interrupted in the area of the 5-membered (F and M) and the six-membered rings H and L, respectively. These ring moieties are non-aromatic as in the corannulene units of **1**; the inner range of the deshielding belt is unexceptionally identifiable based on the ICSS(−0.5 ppm) (deshielding, *orange*) in case of the 5-membered rings F and M, in the six-membered ring moieties H and L, respectively, the inner deshielding belt part portions are not visible due to coverage by the extreme shielding effects above/below the ring levels of the many neighboring aromatic rings.

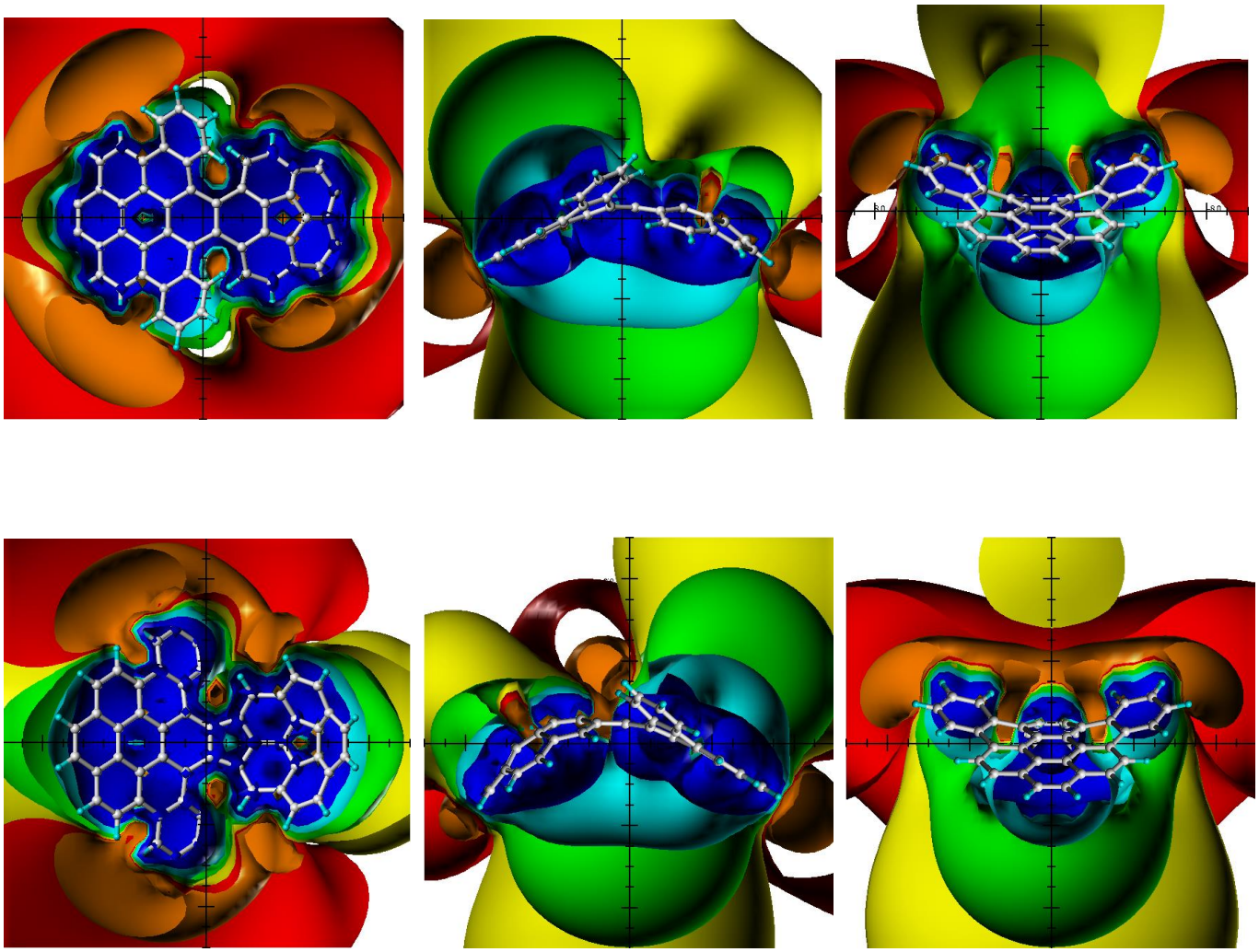

Figure 4. Visualisation of the spatial magnetic properties (TSNMRSs) of **6** (above) and **7** (below) in various views by different ICSS of −0.5 (orange) and −0.1 ppm (red) *deshielding* and 5 ppm (blue), 2 ppm (cyan), 0.5 ppm (green) and 0.1 ppm (yellow) *shielding*.

As a final example of the characterization the aromaticity of polycylic aromatic hydrocarbons on the magnetic criterion, the slightly contorted dinaphthocoronene tetraamide **8** (Scheme 2) was selected which was designed, synthesized und structurally characterized by Tan et al.[28] The common NICS(1)$_{\pi,zz}$ analysis shows strong aromaticity for all benzenoid rings except the central six-membered ring, which is found reduced in aromaticity.[28] The accompanying ACID plot resulted in an outer 34π diatropic and an inner paratropic ring current in accordance with the chemical shifts of the ring protons.[28]

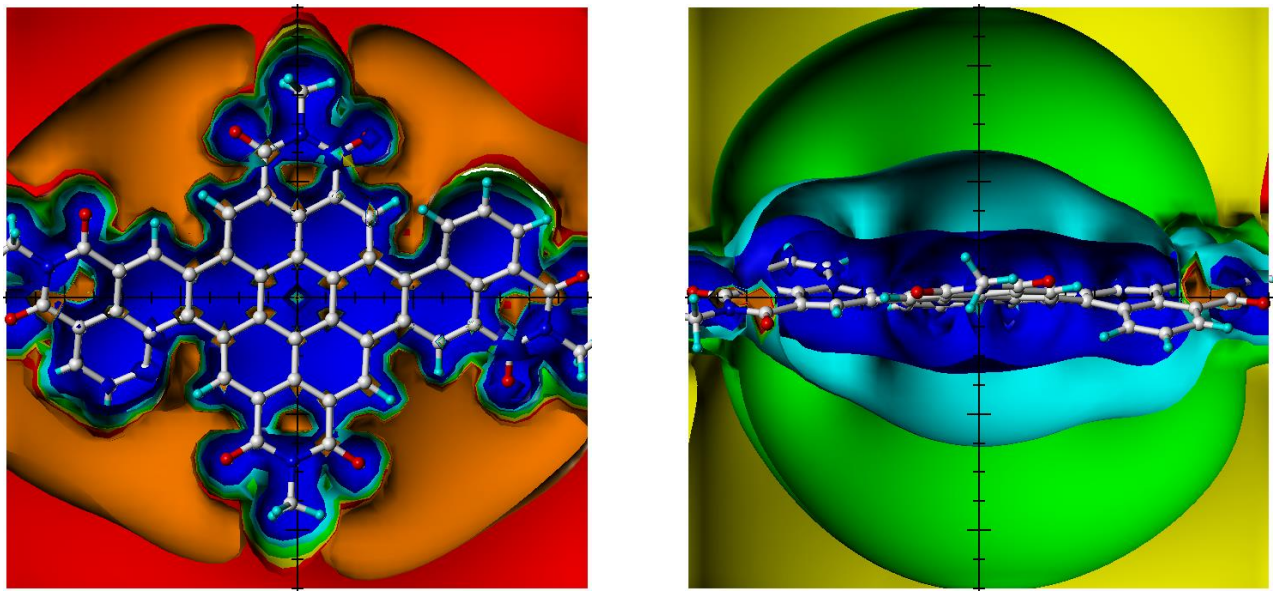

Figure 5. Visualization of the spatial magnetic properties (TSNMRSs) of **8** by different ICSS of −0.5 ppm (orange) and −0.1 ppm (red) *deshielding* and 5 ppm (blue), 2 ppm (cyan), 0.5 ppm (green) and 0.1 ppm (yellow) *shielding*.

The spatial magnetic properties [TSNMRSs, actually the *ring current effect(s)*] of **8** are visualized in Figure 5. First, the aromaticity of the PAH **8** proves to be unequivocally indicated by the peripheral deshielding belt [ICSS(−0.5 ppm), *orange*] and the shielding surfaces [ICSS of +5 (*blue*), +2 (*cyan*) and +0.5 ppm (*green*)] above/below the plane of the only slightly twisted molecule. Further, the ICSS(+5 ppm) surface, *blue*, of **8** never exceed 4.2 Å, the value already known from benzene, and the benzenoid moities of naphthaline or phenanthrene[17,18] – thus, the composition of the PAHs out of benzenoid π-sextets according to Clar´s rule[1] can also be assumed for **8**. The non-aromaticity of the central six-membered ring of **8** can best be recognized also by the ICSS(+5 ppm): The deep incision and the resulting interruption of the ICSS(+5 ppm) surface confirms the lack of involvement of this non-aromatic central 6-membered ring in the π electron delocalization of **8**. Identical results have been obtained for the coronene units in **6** and **7**, and the corannulene units in **1**, **6** and **7** (*vide supra*).

On the other hand, J. Tan et al.[28] found a powerful 34π peripheral diatropic ring current effect in **8**. Its actual existence could also be proven using our TSNMRS method: In the side view of **8**, visualized in Figure 5 (*below, left*), the corresponding ring current effect in the x,z plane is shown. It is dominated by the spatial magnetic properties of the naphthaline moiety of **8**, influenced by the anisotropy/ring current effects of the structural environment. Except ICSS(+5ppm), *blue*, (due to the nonaromaticity of the central 6-membered ring of **8**) the ICSS of +2ppm and +0.5 ppm in **8** (5.2 Å and 10.3 Å, respectively) are significantly larger than in the naphthalene reference (3.5 Å and 6 Å, respectively). This enlargement in **8** can be caused by the existence of the calculated 34π diatropic ring current (and thus its existence could be proven);[28] likewise, both ICSS could also be strengthened among others only by the surrounding pentacene moiety.

For this reason and in order to clear up both options, the underlying PAHs coronene **9**, corannulene **10**, and the corresponding monocyclic analogues **11–13** (Scheme 3) have been additionally and analogously studied (in contrast to [18]annulene **11** the neutral monocyclic π-analogue of corannulene cannot exist, thus, the corresponding [15]annulene cation **12** and anion **13** were calculated instead); the TSNMRSs of these almost close to planar cyclic reference compounds **9–12** are given in Figure 6.

The result proves to be unequivocal: Due to the π-sextet failure of the central six- membered ring in coronene **9** and the five-membered ring in corannulene **10**, respectively, both compounds possess only the limited ring current effect which is composed only of the contributions of the peripheral six-membered benzenoid rings. The [18]annulene **11** and the [15]annulene cation **12** instead can unhinderedly develop the respective 18π and 14π ring current effects; both deshielding belts of **11** and **12** are more pronounced and more intensive [**11:** ICSS(−0.5 ppm) = 9.9 Å, orange; **12** [ICSS(−0.5 ppm) = 8.2 Å, orange] than the corresponding analogues of coronene **9** and corannulene **10** [**9:** ICSS(−0.5 ppm) = 8.5 Å, orange; **10** [ICSS(−0.5 ppm) = 7.0 Å, orange]. The same can be said for the shielding ICSS of +5 to +0.5 ppm (see Figure 5). Again, the ring current effects in **11** and **12** are, comparable to the corresponding deshielding belts, much larger in **11** and **12** and impressively document the losses in the fuselage effects, which result only from the peripheral benzenoid six-membered rings in **9** and **10**, respectively.

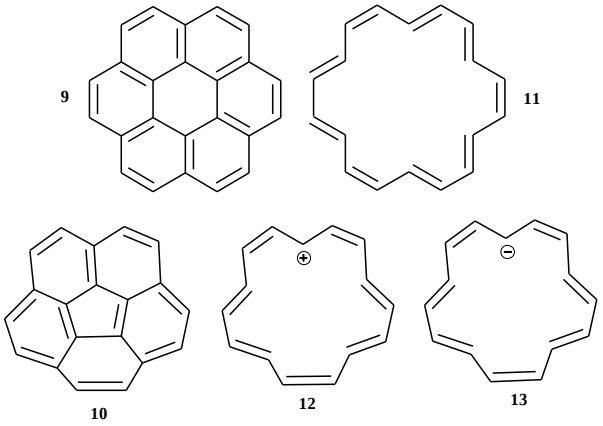

Scheme 3. Polycyclic aromatic hydrocarbons **6–8**.

The [15]annulene anion **13**, due to the 16 conjugated π-electrons, proves to be anti-aromatic and the associated ring current effect to exhibit a shielding belt of remarkable extend in-plane and deshielding ICSSs above/below the slightly twisted (due to steric hindrance of the internal protons) molecule inverse to the ones in **9–12** (see Supporting Information).

Subsequently it can be concluded that polycyclic aromatic hydrocarbons (PAHs) like **1–10** generally consist of conjugated benzenoid 6π-units, the more the more stable the PAH and the more likely the associated resonance contributor, all this in accordance with Clar´s rule.[1] Accordingly , the corresponding ring current effect of PAHs is composed of the sum of the ring current effects of the unique benzenoid moieties and not of a certain peripheral global ring current effect. Remaining non-π-sextets of PAHs are non-aromatic moieties and any paratropic contributions that may be indicated are due to the internal portion of the deshielding belt of the benzenoid units and are not caused by partial antiaromaticity of the non-aromatic ring moiety. If extended aromaticity (10π, 14π, 18-π, etc.) is structurally available (as *e.g.* in annulenes) then more pronounced, correspondingly enlarged ring current effects are measured.

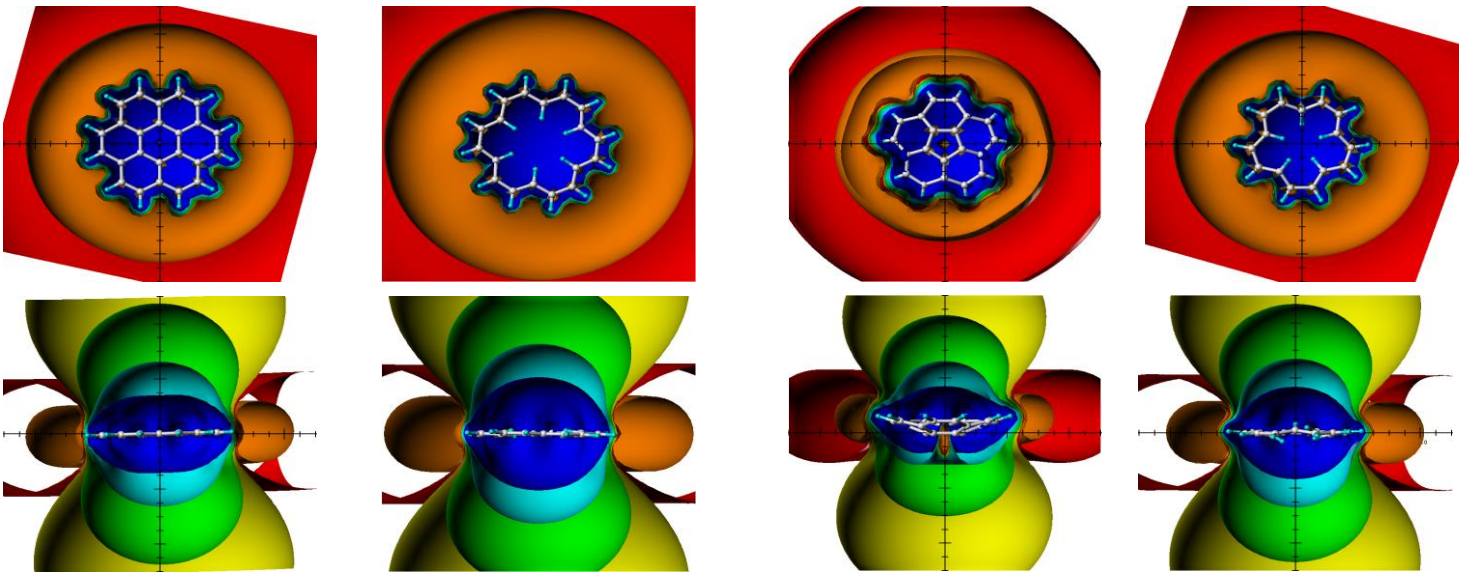

Figure 6. Visualization of the spatial magnetic properties (TSNMRSs) of coronen **9**, [18]annulene **11**, corannulene **10** and [15]annulene$^{(+)}$ **12** by different ICSS of −0.5 ppm (orange) and −0.1 ppm (red) *deshielding* and 5 ppm (blue), 2 ppm (cyan), 0.5 ppm (green) and 0.1 ppm (yellow) *shielding*.

Conclusions

The local and/or global aromaticity of Polycyclic Aromatic Hydrocarbons (PAHs) has been qualified and quantified by the ring current effect in their ^{1}H NMR spectra, which are unique for aromatic compounds. The deshielding belt in-plane of the aromatic moieties and around the periphery of PAHs unequivocally verifies the aromaticity of PAHs at first glance. The shielding areas above/below the plane of mono- and polycyclic aromatic moieties or the whole PAH characterize the extent of detectable aromaticity but also the presence of non-aromatic units within the PAHs both in accordance with Clar´s π-sextet rule.[1] Deshielding areas are only internal contributions of the deshielding belt and do not indicate anti-aromatic units of the PAH. This can often simulate a minor degree of antiaromaticity,[29] especially when the local and/or global aromaticity of PAHs has been qualified and quantified by the ring current effect in their ^{1}H NMR spectra, *e.g.* when five or six aromatic 6π moieties are bonded to a nonaromatic five- or six-membered ring in the center of the molecule, as in coronene and corannulene moieties, respectively.

Experimental Section

The quantum chemical calculations were performed using the Gaussian 09 program package[30] and carried out on LINUX clusters. The studied structures were fully optimized at the B3LYP/6-311G(d,p) level of theory without constraints.[31] The obtained structures have been confirmed as local minima by performing harmonic frequency calculations at the optimized geometries. The calculated structures have been tested for the stability of the wave functions as closed-shell singlets.[32] NICS values[6,7,8] were computed on the basis of the B3LYP/6-311G(*d,p*) geometries using the gauge-including atomic orbital (GIAO) method[33,34] at the B3LYP/6-311G(*d,p*)[35–37] theory level.[38] Variation of the basis set was found to be of non-significant influence on the

NICS values.[17,18] To calculate the spatial NICS, ghost atoms were placed on a lattice of −10 Å to +10 Å with a step size of 0.5 Å in the three directions of the Cartesian coordinate system. The zero points of the coordinate system were positioned at the centers of the studied structures. The resulting 68,921 NICS values, thus obtained, were analyzed and visualized by the SYBYL 7.3 molecular modeling software;[39] different iso-chemical-shielding surfaces (ICSS) of –0.5 ppm (orange) and –0.1 ppm (red) *deshielding*, and 5 ppm (blue), 2 ppm (cyan), 0.5 ppm (green) and 0.1 ppm (yellow) *shielding* were used to visualize the TSNMRSs of the studied structures in the various figures. ICSSs are a quantitative indication of the anisotropy effect in ^{1}H NMR spectroscopy;[16–19] the computed *shielding*(*deshielding*) ICSSs quantify the corresponding ring current effect in ^{1}H NMR spectroscopy subject to the distance from the center of the molecules (in Å).[16–19] Since the SYBYL program is no longer available, the spatial NICS values can also be visualized using GaussView.[40]
External factors, such as solvents used in NMR, temperature, or pressure on the aromaticity results of PAHs were not considered.

Supplementary Material

For the visualization of the spatial magnetic properties (TSNMRS) of the studied compounds **3**, **5** and [15]annulene$^{(-)}$, and the coordinates and absolute energies of the compounds **1–11** studied at the B3LYP/6-311G(d,p) level of theory see Figure S1, S2 and Table S1 in the Supporting Information File associated with this manuscript

References

1. Clar, E. *The Aromatic Sextet*, Wiley 1973.
2. Geuenich, D.; Hess, K.; Köhler, F.; Herges, R. *Chem. Rev.* **2005**, *105*, 3758-3772. https://doi.org/10.1021/cr0300901
3. Dickens, T. K.; Mallion, R. B. *MATCH Commun. Math. Comput. Chem.* **2016**, *76*, 297−356.
4. Sundholm, D.; Dimitrova, M.; Berger, R. J. F. *Chem. Commun.* **2021**, *57*, 12362−12378. https://doi.org/10.1039/D1CC03350F
5. Gershoni-Poranne, R.; Gibson, C. M.; Fowler, P. W.; Stanger, A. *J. Org. Chem.* **2013**, *78*, 7544−7553. https://doi.org/10.1021/jo4011014
6. v. Ragué Schleyer, P.; Maerker, C.; Dransfield, A.; Jiao, H.; van Eikema Hommes, N. J. *J. Am. Chem. Soc.* **1996**, *118*, 6317−6318. https://doi.org/10.1021/ja960582d
7. Chen, C.; Wannere, C. S.; Corminboeuf, C.; Puchta, R.; v. Ragué Schleyer, P. *Chem. Rev.* **2005**, *105*, 3842−3888. https://doi.org/10.1021/cr030088+
8. Fallah-Bagher-Shaidaei, H.; Wannere, C. S.; Corminboeuf, C.; Puchta, R.; v. Ragué Schleyer, P. *Org. Lett.* **2006**, *8*, 863−866. https://doi.org/10.1021/ol0529546
9. Stanger, A. *J. Org. Chem.* **2006**, *71*, 883−893. https://doi.org/10.1021/jo051746o

10. Stanger, A. *Comm.* **2009**, 1939−1947. https://doi.org/10.1039/b816811c
11. Stanger, A. *J. Org. Chem.* **2010**, *75*, 2281−2288. https://doi.org/10.1021/jo1000753
12. Stanger, A. *J. Phys. Chem. A* **2019**,*123*, 3922−3927. https://doi.org/10.1021/acs.jpca.9b02083
13. Stanger, A. *Eur. J. Org. Chem.* **2020**, 3120−3127. https://doi.org/10.1002/ejoc.201901829
14. Gershoni-Poranne, R.; Stanger, A. *Chem. Eur. J.* **2014**, *20*, 5673 – 5688. https://doi.org/10.1002/chem.201304307
15. Artigas, A.; Hagebaum-Reignier, D.; Carissan, Y.; Coquerel, Y. *Chem. Sci.* **2021**, *12*, 13092−13100. https://doi.org/10.1039/D1SC03368A
16. Klod, S.; Kleinpeter, E. *J. Chem. Soc., Perkin Trans. 2* **2001**, 1893−1898.
17. Kleinpeter, E.; Klod, S.; Koch, A. *J. Mol. Struct. (THEOCHEM)* **2007**, *811*, 45−60, and references therein. https://doi.org/10.1016/j.theochem.2007.02.049
18. E. Kleinpeter, *Ann Rep. NMR Spectr.* **2014**, *82*, 115−166. https://doi.org/10.1016/B978-0-12-800184-4.00003-5
19. Kleinpeter, E.; Lämmermann, A.; Kühn, H. *Org. Biomol. Chem*. **2011**, *9*, 1098−1111. https://doi.org/10.1039/C0OB00356E
20. Kleinpeter, E.; Koch, A. *Tetrahedron* **2011**, *67*, 5740−5743. https://doi.org/10.1016/j.tet.2011.06.005
21. Xu, Q.; Wang, C.; Zheng, D.; He, J.; Wang, Y.; Chen, X.; Jiang, H. *J. Org. Chem.* **2021**, *86*, 13990−13996. https://doi.org/10.1021/acs.joc.0c03065
22. Dickens, T. K.; Mallion, R. B. *J. Org. Chem.* **2021**, *86*, 17404−17408. https://doi.org/10.1021/acs.joc.1c01836
23. Steiner, E.; Fowler, P. W.; Jenneskens, L. W. *Angew. Chem. Int. Ed.* **2001**, *40*, 363−366. https://doi.org/10.1002/1521-3773(20010119)40:2<362::AID-ANIE362>3.3.CO;2-Q
24. Lazzeretti, P. *Phys. Chem. Chem. Phys.* **2004**, *6*, 217−223. https://doi.org/10.1039/B311178D
25. Pelloni, St.; Lazzeretti, P.; Zanasi, R. *J. Phys. Chem. A* **2007**, *111*, 8163−8169. https://doi.org/10.1021/jp0710638
26. Wei, L.; Deng, X.; Yu, X.; Li, X.; Wang, W.; Zhang, C.; Xiao, J. *J. Org. Chem.* **2021**, *86*, 17535−17542. https://doi.org/10.1021/acs.joc.1c00989
27. Xu, Q.; Wang, C.; Zhao, Y.; Zheng, D.; Shao, C.; Guo, W.; Deng, X.; Wang, Y.; Chen, X.; Zhu, J.; Jiang, H. *Org. Lett.* **2020**, *22*, 7397−7402. https://doi.org/10.1021/acs.orglett.0c02754
28. Tan, J.; Zhang, G.; Ge, C.; Liu, J.; Zhou, L.; Liu, C.; Gao, X.; Narita, A., Zou, Y.; Hu, Y. *Org. Lett.* **2022**, *24*, 2414−2419. https://doi.org/10.1021/acs.orglett.2c00690
29. Kleinpeter, E.; Koch, A. *Org. Biomol. Chem.* **2024**, *22*, 3035–3044. https://doi.org/10.1039/D4OB00114A
30. Frisch, M. J.; Trucks, G. W.; Schlegel, H. B.; Scuseria, G. E.; Robb, M. A.; Cheeseman, J. R.; Scalmani, G.; Barone, V.; Mennucci, B.; Petersson G. A. et al. Gaussian 09, Revision D.01; Gaussian, Inc.: Wallingford, CT, 2009.

31. Hehre, W. J.; Radom, L.; v. Ragué Schleyer, P.; Pople, J. A. *Ab initio Molecular Orbital Theory*, Wiley: New York, 1986.
32. Bendikov, M.; Duong, H. M.; Starkey, K.; Houk, K. N.; Carter, E. A.; Wudl, F. *J. Am. Chem. Soc.* **2004**, *126*, 7416−7417. https://doi.org/10.1021/ja048919w
33. Ditchfield, R. *Mol. Phys.* **1974**, *27*, 789−807. https://doi.org/10.1080/00268977400100711
34. Cheeseman, G. W.; Trucks, T. A.; Keith, M. J. A. *J. Chem. Phys.,* **1996**, *104*, 5497−5509. https://doi.org/10.1063/1.471789
35. Becke, A. D. *J. Chem. Phys.,* **1993**, *98*, 5648−5652. https://doi.org/10.1063/1.464913
36. Lee, C.; Yang, W.; Parr, R. G. *Phys. Rev. B,* **1988**, *37*, 785−789. https://doi.org/10.1103/PhysRevB.37.785
37. Miehlich, B.; Savin, A.; Stoll, H.; Preuss, H. *Chem. Phys. Lett.,* **1989**, *157*, 200−206. https://doi.org/10.1016/0009-2614(89)87234-3
38. The lattice points ("*ghost atoms*") should be sensor points only without energy contribution in the present calculations. Only if DFT or HF calculations are applied this is true; in case of electron correlation calculations, the "ghost atoms" get their own electron density and show some influence on the energy of the studied molecule. In these cases, the TSNMRS surfaces are heavily distorted.
39. SYBYL 7.3 Tripos Inc., 1699 South Hanley Road, St. Louis, Missouri 63144, USA, 2007.
40. *GaussView*: Gaussian Inc. 340 Quinnipiac St. Bldg. 40, Wallingford, CT 06492, USA.

